Geometric approach to viscous fingering on a cone

2003 J. Phys. A: Math. Gen. 36 863

(http://iopscience.iop.org/0305-4470/36/3/319)

INSTITUTE OF PHYSICS PUBLISHING JOURNAL OF PHYSICS A: MATHEMATICAL AND GENERAL

J. Phys. A: Math. Gen. **36** (2003) 863–874 PII: S0305-4470(03)52252-1

Geometric approach to viscous fingering on a cone

José A Miranda and Fernando Moraes

Laboratório de Física Teórica e Computacional, Departamento de Física, Universidade Federal de Pernambuco, Recife, PE 50670-901 Brazil

Received 2 August 2002, in final form 20 November 2002
Published 7 January 2003
Online at stacks.iop.org/JPhysA/36/863

Abstract

We study fluid flow and the formation of viscous fingering patterns on a two-dimensional conical background space, defined as the conical Hele–Shaw cell. We approach the problem geometrically and study how the nontrivial topological structure of the conical cell affects the evolution of the interface separating two viscous fluids. We perform a perturbative weakly nonlinear analysis of the problem and derive a mode-coupling differential equation which describes fluid–fluid interface behaviour. Our nonlinear study predicts the formation of fingering structures in which fingers of different lengths compete and split at their tips. The shape of the emerging patterns show a significant sensitivity to variations in the cell's topological features, which can be monitored by changing the cone opening angle. We find that for increasingly larger values of the opening angle, finger competition is inhibited while finger tip-splitting is enhanced.

PACS numbers: 47.20.Ma, 02.40.−k, 61.72.Lk

1. Introduction

The use of topological and geometrical tools in theoretical physics has been steadly increasing in the past few decades. Topology and geometry play an important role in a wide spectrum of interdisciplinary fields in physics, ranging from gravitation theory to condensed matter. In particular, topological defects are a good example of this. They appear in gravitation as monopoles, strings and walls [1]. In condensed matter systems these defects arise as vortices in superconductors [2], solitons in effectively one-dimensional polymers [3], and as disclinations or dislocations in solid and liquid crystals [4]. In this work we adapt a geometric approach ordinarily used to study topological defects in solids to analyse the pattern formation at the interface separating two viscous fluids in a nonplanar two-dimensional setting.

A decade ago Katanaev and Volovich [1] proposed an interesting mapping between the theory of defects in solids and three-dimensional gravity: for instance, they viewed a disclination, a defect in an elastic solid, as the analogue of a cosmic string in spacetime.

The analogy suggested in [1] goes beyond topology: in some cases of interest [5] both kinds of defects can be treated by the same geometric methods. Within this approach, known as the geometric theory of defects, the introduction of a disclination is equivalent to the creation of a conical singularity in the otherwise smooth background. This singularity appears as a result of a Volterra process [4] of cutting out a sector of the space and identifying the loose ends. This essentially topological process is based on ideas of the homology theory [6]. Therefore, a medium containing defects may be described by a simple two-dimensional metric, associated with a locally flat environment with a conical singularity at the origin. This geometric approach has been proved to be a promising and useful tool to attack a number of physical problems in condensed matter, gravitation and cosmology [5, 7–13].

We use the general ideas developed by Katanaev and Volovich, and extend their applicability to the realm of fluid mechanics. We investigate the motion and pattern formation dynamics associated with the flow of viscous fluids on a conical background space. More precisely, we examine the viscous fingering Saffman–Taylor problem [14] on a cone. This celebrated hydrodynamic problem [14, 15] arises when a less viscous fluid pushes a more viscous one in the thin gap between two flat parallel plates (a device known as the Hele–Shaw cell). The less viscous fluid can either be injected at an end of a channel-shaped cell (rectangular setup) [14, 15], or from the centre of the cell (radial setup) [16]. The moving interface separating the fluids becomes unstable, leading to the formation of a wide variety of patterns—from stable smooth fingers to highly branched, fractal-like structures. These complex finger-like patterns have been studied in great detail during their linear [14, 16], weakly nonlinear [17, 18] and fully nonlinear stages [15] of evolution. The morphology of the patterns is well described by the basic mechanisms of finger tip-splitting and finger competition [15].

Viscous fingering is a Laplacian growth process, so the motion of the fluid–fluid interface depends upon the boundary conditions governed by the shape of the Hele–Shaw cell. Research in the field is practically restricted to the study of confined viscous flow in *flat* backgrounds (flat Hele–Shaw cells) [14–18]. Remarkably, only very recently researchers performed systematic theoretical investigations of the Saffman–Taylor flow in more complex, *nonflat* surroundings, such as flow in spherical [19] and cylindrical [20] Hele–Shaw cells. These studies reveal that the two-fluid interface behaviour is coupled to the geometry of the nonflat Hele–Shaw cell, so that cell curvature has important consequences for flow dynamics.

In this paper we carry out a detailed study of the viscous fingering phenomenon on a *conical* background space (conical Hele–Shaw cell). Such a conical environment is formed by a pair of coaxial, narrowly spaced, thin conical shells, having the same opening angle. In contrast to spherical [19] and cylindrical [20] cases, instead of concentrating on purely geometrical effects due to cell curvature, we need to take into account the combined influence of cell *geometry* and *topology* on the interface dynamics. To accomplish this, and inspired by the work of Katanaev and Volovich [1], we propose a simple analytical approach that is ideally suited to bringing out both geometrical and topological aspects related to viscous fluid flow in narrow conical passages.

The paper is organized as follows: section 2 defines viscous flow in a conical geometry. We formulate our geometric approach, based on a simple two-dimensional metric which introduces an appropriate redefinition of the angular variable periodicity. We perform a Fourier decomposition of the interface shape and derive coupled, nonlinear, ordinary differential equations governing the time evolution of Fourier amplitudes. Section 3.1 discusses both linear and weakly nonlinear interface evolution for a fixed cone opening angle, considering the coupling of various modes. Section 3.2 concentrates on the effect of varying opening angle 2γ on finger tip-splitting and finger competition. We show that increasingly larger values of

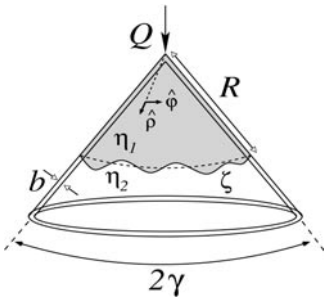

Figure 1. Schematic illustration of viscous flow on a cone (conical Hele–Shaw cell). The cone opening angle is 2γ. The unit vectors $\hat{\rho}$ and $\hat{\varphi}$ point in the direction increasing ρ and φ, respectively. See the text for a complete definition of all relevant physical quantities.

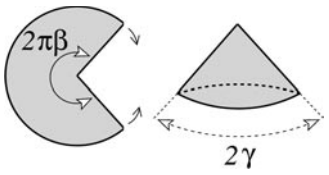

Figure 2. A two-dimensional, flat disc with a wedge of angle $2\pi(1-\beta)$ removed has the intrinsic geometry of a cone rather than that of a plane. By identifying the two resulting edges, one obtains a conical surface of opening angle 2γ, which is locally flat everywhere except at the cone's vertex. The cone opening angle is related to the parameter β by $\beta = \sin\gamma$.

2γ inhibit competition and enhance splitting. Section 4 summarizes our chief conclusions and presents our final remarks.

2. Basic formalism and governing equations

Consider two immiscible, incompressible, viscous fluids, flowing in a narrow gap between two coaxial, thin conical shells (figure 1). Both shells have the same opening angle 2γ resulting in a constant gap thickness b between them. We refer to this apparatus as the *conical* Hele–Shaw cell. Assume that b is smaller than any other length scale in the problem, so the system is effectively two dimensional. The flow takes place in a two-dimensional surface, embedded in three-dimensional space, so it is convenient to work in polar coordinates (ρ, φ), with the metric [1]

$$\mathrm{d}s^2 = \mathrm{d}\rho^2 + \rho^2\,\mathrm{d}\varphi^2 \tag{1}$$

where $0 \leqslant \rho < \infty$ is the distance from the radial flow source, located at the apex of the cone ($\rho = 0$), and $0 \leqslant \varphi \leqslant 2\pi\beta$ denotes the polar angle measured on the cone, where $0 < \beta \leqslant 1$. Note the change in the periodicity of the azimuthal angle φ from the usual value of 2π to $2\pi\beta$ in equation (1). This somewhat unconventional change in φ is intrinsically related to the conical nature of the space on which the flow takes place. The space defined by metric (1) is obtained by cutting out a wedge of angle $2\pi(1-\beta)$ from a planar surface, and identifying the resulting edges. The result is a cone of opening angle 2γ, where $\beta = \sin\gamma$. This 'cut-and-glue' process is illustrated in figure 2. The cone described by (1) is locally flat with a conical singularity at its vertex [21, 22]. It can be shown that the Gaussian curvature of the cone is given by $K = 2\pi(1-\beta)\delta_2(\rho)$, where $\delta_2(\rho)$ is the two-dimensional delta function [23, 24].

At any stage of our calculation, the 'flat-cell' limit $\beta \to 1$ (or, equivalently, $2\gamma \to \pi$) gives all the well-known familiar results for radial flow in *flat* Hele–Shaw cells [16].

A conical Hele–Shaw cell is in fact flat, since the Gaussian curvature of the cone vanishes everywhere except at the vertex, which is removed in order to provide an inlet for the fluids. Nevertheless, a 'memory' of the singularity remains in the $2\pi\beta$ periodicity of the azimuthal angle. So, it is of interest to investigate how the nontrivial geometrical and topological features of the cell affect interfacial pattern formation. We choose to examine such effects by using the parameter β. This parameter measures how sharp the cone is, as well as the intensity of the curvature at the cone's vertex. By varying β we change an intrinsic topological property of the conical Hele–Shaw cell—the deficit angle, or the angular aperture of the missing wedge. In addition, from a practical point of view it is convenient to describe things in terms of β, since it is easily related to the experimentally accessible control parameter 2γ. Eventually, laboratory investigations using conical cells could monitor the effects of varying β, by performing experiments in cells of different opening angles 2γ.

Denote the viscosities of the upper and lower fluids, respectively, as η_1 and η_2 (figure 1). Fluid 1 is injected into fluid 2 through an inlet located at the cone's vertex, at a given flow rate Q, which is the area covered per unit time. Immiscibility implies that there exists a surface tension σ between the fluids. The flows are assumed to be irrotational, except at the interface. During the flow, the two-fluid interface has a perturbed shape described as $\rho \equiv \mathcal{R}(\varphi, t) = R + \zeta(\varphi, t)$, where $R = R(t)$ denotes the time-dependent unperturbed radius, and $\zeta(\varphi, t)$ represents the interface perturbation amplitude. We neglect the acceleration due to gravity and focus on the interplay between the viscosity-driven instability and cell topology.

Fluid flow in the confined geometry of a Hele–Shaw cell is viscous dominated and inertial effects are neglected. Under such circumstances the two-dimensional fluid velocity is given by Darcy's law [14, 15]:

$$\mathbf{v}_j(\rho, \varphi) = -\frac{b^2}{12\eta_j}\nabla p_j(\rho, \varphi) \tag{2}$$

where p_j denotes the pressure in fluids $j = 1$ and 2. We make use of the irrotational flow condition to define the velocity potential $\mathbf{v}_j = -\nabla\phi_j$. The incompressibility of the fluids $\nabla \cdot \mathbf{v}_j = 0$ means that the velocity potentials satisfy Laplace's equation $\nabla^2\phi_j = 0$. The problem is then specified by two boundary conditions at the interface: (i) $(p_1 - p_2)|_{\mathcal{R}} = \sigma\kappa|_{\mathcal{R}}$, which expresses the pressure jump at the interface, where κ denotes the intra-surface interface curvature; (ii) the kinematic boundary condition $\mathbf{n} \cdot \mathbf{v}_1|_{\mathcal{R}} = \mathbf{n} \cdot \mathbf{v}_2|_{\mathcal{R}}$, which states that the normal components of each fluid's velocity are continuous at the interface [25]. The vector $\mathbf{n}$ denotes the unit normal to the interface pointing from fluid 1 to fluid 2.

Rewrite equation (2) for fluid 1 in terms of the velocity potential, subtract it from the equivalent equation for fluid 2, and divide by the sum of the two fluids' viscosities. Then, combine the resulting expression with equation for the pressure difference. This yields an equation for the discontinuity of velocity potentials valid at the two-fluid interface

$$A\left(\frac{\phi_1|_{\mathcal{R}} + \phi_2|_{\mathcal{R}}}{2}\right) - \left(\frac{\phi_1|_{\mathcal{R}} - \phi_2|_{\mathcal{R}}}{2}\right) = -\alpha\kappa \tag{3}$$

where $A = (\eta_2 - \eta_1)/(\eta_2 + \eta_1)$ is the viscosity contrast and $\alpha = b^2\sigma/[12(\eta_1 + \eta_2)]$. Our main task is to write $\phi_j|_{\mathcal{R}}$ and κ in equation (3) in terms of the interface perturbation amplitude $\zeta(\varphi, t)$ and derive a differential equation describing its time evolution.

To investigate the linear and early nonlinear evolution of the two-fluid interface in a conical Hele–Shaw cell, we represent the net interface perturbation as

$$\zeta(\varphi, t) = \sum_{n=-\infty}^{+\infty} \zeta_n(t) \exp\left(\frac{\mathrm{i}n\varphi}{\beta}\right) \tag{4}$$

where $\zeta_n(t) = (1/2\pi\beta)\int_0^{2\pi\beta} \zeta(\varphi, t)\exp[-\mathrm{i}n\varphi/\beta]\,\mathrm{d}\varphi$ denotes the complex Fourier mode amplitudes and $n = 0, \pm1, \pm2, \ldots$, is the discrete azimuthal wave number. In our Fourier expansion (4) we include the $n = 0$ mode to keep the area of the perturbed shape independent of the perturbation ζ. Mass conservation imposes that the zeroth mode is written in terms of the other modes as $\zeta_0 = -(1/2R)\sum_{n\neq0}|\zeta_n(t)|^2$, that is independent of β.

Now define Fourier expansions for the velocity potentials ϕ_j. Far from the interface the velocity field should approach the unperturbed steady flow with a circular interface of radius R. Thus for $\rho \to 0$ and $\rho \to +\infty$ the velocity potentials ϕ_j approach ϕ_j^0, the velocity potentials for radial flow

$$\phi_j^0 = -\frac{Q}{2\pi\beta}\log\left(\frac{\rho}{R}\right) + D_j. \tag{5}$$

D_j are independent of ρ and φ. From equation (5) we easily verify that the unperturbed interface velocity $v = Q/L$, where $L = 2\pi\beta R$ denotes the unperturbed interface perimeter. The general velocity potentials obeying the requirements mentioned above are

$$\phi_1 = \phi_1^0 + \sum_{n\neq0}\phi_{1n}(t)\left(\frac{\rho}{R}\right)^{\frac{|n|}{\beta}}\exp\left(\frac{\mathrm{i}n\varphi}{\beta}\right) \tag{6}$$

and

$$\phi_2 = \phi_2^0 + \sum_{n\neq0}\phi_{2n}(t)\left(\frac{R}{\rho}\right)^{\frac{|n|}{\beta}}\exp\left(\frac{\mathrm{i}n\varphi}{\beta}\right). \tag{7}$$

To calculate the mode coupling differential equation for the system, we substitute expansions (5), (6) and (7) into the equation of motion (3), keep second-order terms in the perturbation amplitudes, and Fourier transform them. However, we still need additional relations expressing the velocity potentials in terms of the perturbation amplitudes. To find these, expand the kinematic boundary condition to second order in ζ and then Fourier transform. Solving for $\phi_{jn}(t)$ consistently to second order in ζ yields

$$\begin{aligned}\phi_{1n}(t) = {} & -\frac{R\beta}{|n|}\dot{\zeta}_n - \frac{Q}{2\pi R|n|}\zeta_n + \sum_{n'\neq0}\left(\mathrm{sgn}(nn') - \frac{\beta}{|n|}\right)\dot{\zeta}_{n'}\zeta_{n-n'} \\ & + \frac{Q}{2\pi R^2\beta}\sum_{n'\neq0}\mathrm{sgn}(nn')\zeta_{n'}\zeta_{n-n'}\end{aligned} \tag{8}$$

and a similar expression for $\phi_{2n}(t)$. The overdot denotes total time derivative. The sgn function equals ±1 according to the sign of its argument.

We can use relation (8) to replace the velocity potential ϕ_1 in the equation of motion (3) with the perturbation ζ and its time derivative $\dot{\zeta}$. The same procedures are repeated for fluid 2. Keeping only quadratic terms in the perturbation amplitude, and equating Fourier modes n on each side of equation (3), leads to the differential equation for perturbation amplitudes ζ_n. For $n \neq 0$,

$$\dot{\zeta}_n = \lambda(n)\zeta_n + \sum_{n'\neq0}[F(n, n')\zeta_{n'}\zeta_{n-n'} + G(n, n')\dot{\zeta}_{n'}\zeta_{n-n'}] \tag{9}$$

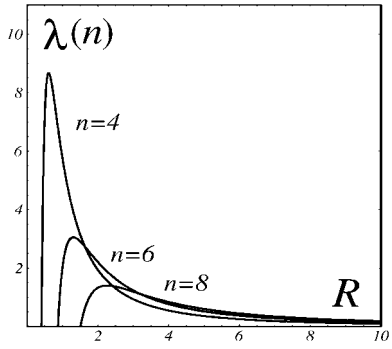

Figure 3. Variation of the linear growth rate (equation (10)) as a function of the unperturbed interface radius R, for modes $n = 4, 6, 8$, and cone opening angle $2\gamma = \pi/2$.

where

$$\lambda(n) = \left[\frac{Q}{2\pi R^2\beta^2}(A|n| - \beta) - \frac{\alpha}{R^3\beta}|n|\left(\frac{n^2}{\beta^2} - 1\right)\right] \tag{10}$$

denotes the linear growth rate, and

$$F(n, n') = \frac{|n|}{R}\left\{\frac{QA}{2\pi R^2\beta^2}\left[\frac{1}{2} - \mathrm{sgn}(nn')\right] - \frac{\alpha}{R^3\beta}\left[1 - \frac{n'}{2\beta^2}(3n' + n)\right]\right\} \tag{11}$$

$$G(n, n') = \frac{1}{R}\left\{A\frac{|n|}{\beta}[1 - \mathrm{sgn}(nn')] - 1\right\} \tag{12}$$

represent second-order mode coupling terms. Equation (9) is the mode coupling equation of the Saffman–Taylor problem on a cone. It gives us the time evolution of the perturbation amplitudes ζ_n, accurate to second order, in terms of the 'topological' parameter β. The rest of the paper uses equation (9) to study the development of the viscous fingering instability in conical Hele–Shaw cells, and to examine how the cell's topology affects pattern morphology.

3. Discussion

3.1. Linear and weakly nonlinear evolution

In this section we study both linear and nonlinear interface evolutions, considering a conical Hele–Shaw cell of *fixed* opening angle. In section 3.2 we analyse the effects of *changing* β on the mechanisms of finger tip-splitting and finger competition.

To examine the linear stage of the interface evolution, we consider the first term on the right-hand side of equation (9). The development of the linear instability may be described by integrating the growth rate of each Fourier mode n as a function of time. Since the unperturbed radial position R is time dependent, the interface is unstable if $\int_0^t \lambda(n)\,\mathrm{d}t' > 0$. To gain an insight about the linear growth, we plot in figure 3 the variation of the growth rate (10) for a few values of n as a function of R, for a conical cell of opening angle $\pi/2$ (or $\beta = \sqrt{2}/2$). Throughout the text we use the experimental parameters given in Paterson's classical, radial flow experiment in flat cells [16]. Paterson observed growth of bifurcating, viscous fingering patterns, as air ($\eta_1 \approx 0$) was blown at constant injection rate $Q = 9.3\,\mathrm{cm}^2\,\mathrm{s}^{-1}$, into glycerine ($\eta_2 \approx 5.21\,\mathrm{g/(cm\,s^{-1})}$) in a radial setup. The thickness of the cell $b = 0.15$ cm and the surface tension $\sigma = 63\,\mathrm{dyne/cm}$.

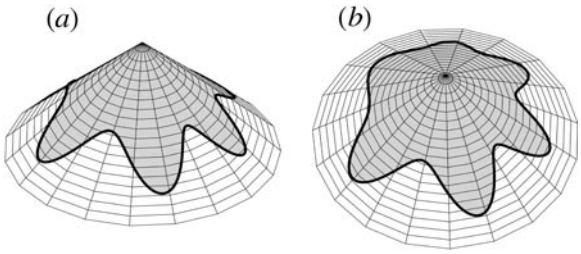

Figure 4. Time evolution of the two-fluid interface according to the linear solution (equation (14)). We show the fluid–fluid interface at $t = 15$ s, from two different perspectives: (*a*) front view, and (*b*) upper view.

Figure 3 shows that, for sufficiently small values of R, all modes are stabilized by surface tension. As the interface advances outward, different modes become unstable at different radial positions. So, for each n there exists a critical radius (when $\lambda(n) = 0$) at which the interface becomes unstable

$$R_c(n) = \frac{2\pi\alpha}{Q\beta}\frac{|n|(n^2-\beta^2)}{(A|n|-\beta)}. \tag{13}$$

It is clear from figure 3 that each Fourier mode n has very different growth rates as the value of R varies. For a given n, $\lambda(n)$ increases to a maximum value and subsequently decays, although remaining positive. Therefore, the fastest growing mode (defined by setting $\mathrm{d}\lambda(n)/\mathrm{d}n = 0$) gradually increases as R increases. As a result, at the linear stage there is a cascade to higher modes as the interface evolves.

Following [18], we assume the presence of a constant low level of noise during the whole evolution of the interface. For a given mode n the perturbation amplitude ζ_n starts to vary with time only when the corresponding $R_c(n)$ is reached. Within this model, we write the first-order (linear) solution of equation (9) as

$$\zeta_n^{\mathrm{lin}}(t) = \begin{cases} \zeta_n(0) & \text{for} \quad R < R_c(n) \\ \zeta_n(0)\left\{\left(\frac{R}{R_c(n)}\right)^{\left(A\frac{|n|}{\beta}-1\right)} \exp\left[\left(A\frac{|n|}{\beta}-1\right)\left(\frac{R_c(n)}{R}-1\right)\right]\right\} & \text{for} \quad R \geqslant R_c(n). \end{cases} \tag{14}$$

To see the overall effect of the linear solution equation (14), we plot the time evolution of the interface in figure 4. For convenience we rewrite the net perturbation (4) in terms of cosine and sine modes

$$\zeta(\varphi, t) = \zeta_0 + \sum_{n=1}^{\infty}\left[a_n(t)\cos\left(\frac{n\varphi}{\beta}\right) + b_n(t)\sin\left(\frac{n\varphi}{\beta}\right)\right] \tag{15}$$

where $a_n = \zeta_n + \zeta_{-n}$ and $b_n = \mathrm{i}(\zeta_n - \zeta_{-n})$ are real-valued. We take into account modes n ranging from $n = 2$ up to 20 and set the cone opening angle as $\pi/2$. We evolve from initial radius $R_0 = 0.05$ cm and the noise amplitude $|\zeta_n(0)| = R_0/1100$. To facilitate visualization figures 4(*a*) and (*b*) show the evolution of the interface from two distinct viewpoints, for a random choice of phases, up to time $t = 15$ s. We observe the development of fingers of different lengths, indicating finger competition. The longer fingers present somewhat narrow tips that show no tendency to split. Purely linear analysis may mimic finger competition, but it fails to reproduce tip-splitting events.

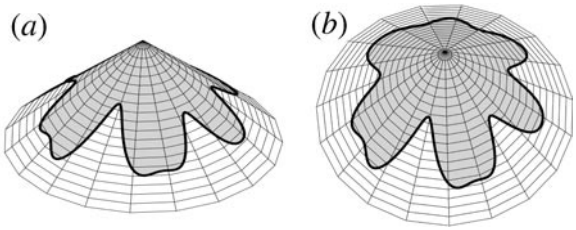

Figure 5. Interface evolution according to the nonlinear solution (equation (16)). All physical parameters, initial conditions, and viewpoints are the same as those used in figure 4.

Now we turn our attention to the weakly nonlinear evolution. To visualize the consequences of the second-order term in the equations of motion, we solve equation (9) to second-order accuracy. We linearize equation (9) and obtain a first-order differential equation with solution

$$\zeta_n(t) = \begin{cases} \zeta_n(0) & \text{for} \quad R < R_c(n) \\ \zeta_n^{\text{lin}}(t)\left[1 + \int_{t_c(n)}^{t} I(n,t')\,\mathrm{d}t'\right] & \text{for} \quad R \geqslant R_c(n) \end{cases} \tag{16}$$

where

$$I(n,t') = \frac{\sum_{n'\neq 0}\left[F(n,n')\zeta_{n'}^{\text{lin}}(t')\zeta_{n-n'}^{\text{lin}}(t') + G(n,n')\dot{\zeta}_{n'}^{\text{lin}}(t')\zeta_{n-n'}^{\text{lin}}(t')\right]}{\zeta_n^{\text{lin}}(t')} \tag{17}$$

and $t_c(n)$ is the time required for the unperturbed growth to reach radius $R_c(n)$.

We use the second-order solution (16) to investigate the nonlinear coupling among various modes n. In figures 5(a) and (b), we plot the interface for a certain time ($t = 15$ s), considering the same random choice of initial phases and viewpoints as was employed in figure 4, and coupling all modes with $2 \leqslant n \leqslant 20$. By comparing figures 4 and 5 we verify that nonlinear evolution results in interface shapes which are clearly different from those obtained from purely linear analysis. Typically, nonlinear fingers are wider and their tips are flatter. For some of the fingers the flat tip becomes an indentation leading to tip-splitting formation. Finger competition is also evident. It is reassuring to note that for a fixed conical cell angle our theoretical approach is capable of capturing typical nonlinear behaviour detected in flat Hele–Shaw cells. However, the most interesting effects arise when the cell opening angle is varied. We analyse pattern behaviour under variable opening angle conditions in the next subsection.

3.2. Opening angle effects on tip-splitting and finger competition

In this section we study how variations in the parameter β (or equivalently, in the cone opening angle 2γ) influence finger tip-splitting and finger competition. To accomplish this we use equation (9) to investigate the coupling of a small number of modes.

Flow in conical cells involves many parameters, so one must exercise caution in handling with situations in which β is varied. It is important to change only one relevant quantity at a time to see what each one does. We want to isolate the influence of β from the effect of variations in the unperturbed interface velocity v and the unperturbed interface contour length L. Following Parisio *et al* [19] we adopt an instantaneous approach: we look at the linear growth rate and mode coupling at an instant in time, ignoring the past history of how a given interface arose from some initial condition followed by growth. Such an instantaneous

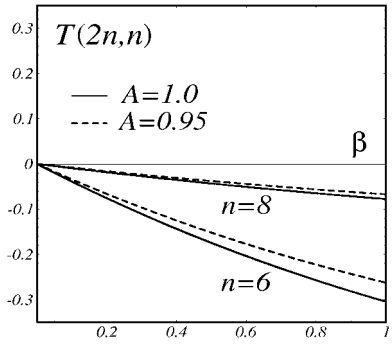

Figure 6. Variation of $T(2n, n)$ as a function of β, for Fourier modes $n = 6, 8$. The solid (dashed) curves describe evolution for $A = 1$ ($A = 0.95$).

approach, at which L and v have a particular value, enables us to compare the behaviour of interfaces evolving for different values of β, but under dynamically equivalent circumstances. The identity $Q = vL$ holds, such that the injection rate Q in the flat cell equals Q in conical cells, regardless the value of the cell opening angle under consideration.

First, let us analyse finger tip-splitting behaviour when β is varied. Tip-splitting is related to the influence of a fundamental mode n on the growth of its harmonic $2n$ [18]. To observe interfacial instability of the fundamental mode n, we must have $\lambda(n) > 0$. In addition, to allow growth of the harmonic mode $2n$ we assume that $\lambda(2n) > 0$. Without loss of generality we may choose the phase of the fundamental mode so that $a_n > 0$ and $b_n = 0$. We replace the time derivative terms $\dot{a}_n$ and $\dot{b}_n$ by $\lambda(n)a_n$ and $\lambda(n)b_n$, respectively, for consistent second-order expressions. Under these circumstances the equations of motion for the harmonic mode become

$$\dot{a}_{2n} = \lambda(2n)a_{2n} + \tfrac{1}{2}T(2n, n)a_n^2 \tag{18}$$

$$\dot{b}_{2n} = \lambda(2n)b_{2n} \tag{19}$$

where the tip-splitting function is defined as

$$T(2n, n) = [F(2n, n) + \lambda(n)G(2n, n)]. \tag{20}$$

The sign of $T(2n, n)$ in equation (18) dictates finger tip-splitting behaviour. If $T(2n, n) < 0$, the result is a driving term of order a_n^2 forcing growth of $a_{2n} < 0$. With this particular phase of the harmonic forced by the dynamics, the n outwards-pointing fingers of the fundamental mode n tend to split. Note that growth of sine mode b_{2n} is uninfluenced by b_n.

We want to monitor the effect of varying β on finger tip-splitting. We consider a particular v and L combination at the onset of growth of mode $2n$ (using the condition $\lambda(2n) = 0$) in the flat cell limit $\beta \to 1$, where it is known that $T(2n, n) < 0$ [18]. To illustrate how tip-splitting varies with opening angle, we plot in figure 6 the function $T(2n, n)$ with respect to β. The solid curves refer to viscosity contrast $A = 1$, while the dashed curves are obtained by considering a slightly smaller value $A = 0.95$. We see that, for a given n, the magnitude of $T(2n, n)$ is maximum for the flat, radial case ($\beta = 1$) and decreases as β tends to zero. Consequently, tip-splitting is enhanced for increasingly larger values of the cell opening angle 2γ. The wider the conical cell, the stronger the tendency towards tip-splitting. By inspecting the behaviour of $T(2n, n)$ for different values of n in figure 6, we conclude that the larger the number of fingers, the weaker the intensity of the driving force leading to the splitting of their tips. We also note that finger tip-splitting is enhanced to a degree proportional to A.

Apparently, the conclusion that increasing the opening angle favours the tendency towards tip-splitting may seem not very surprising. However, we stress it should not be taken for granted: if on one hand wider cells (larger β values) provide more room for the fingers to split, on the other, for fixed Q the interface unperturbed velocity v decreases with increasing β, what would inhibit interfacial instability. It is well known that finger tip-splitting is a purely nonlinear phenomenon [18], so its behaviour under varying cell opening angles could defy intuition. The enhanced propensity for tip-splitting in wider conical cells captured by our geometric approach is a careful verification of such a nontrivial aspect related to the shape of the emerging patterns.

It is interesting to contrast finger tip-splitting behaviour in conical cells with its equivalent in spherical [19] and cylindrical [20] geometries. In [19] it has been shown that tip-splitting is sensitive to the Gaussian curvature, K, of the nonplanar cell: flow in positively curved Hele–Shaw cells ($K > 0$) presenting increasingly larger curvature, would lead to suppression of finger tip-splitting in comparison with that observed in radial, flat cells ($K = 0$). We recall that a cone presents a nonzero Gaussian curvature associated with its apical singularity. It turns out that such curvature, concentrated at the cone's vertex, depends on β [23, 24], and increases as β (or, equivalently the cone opening angle 2γ) decreases. Motivated by the latter, and the results obtained in [19], one would expect that in conical cells tip-splitting would be inhibited as β is decreased. This is exactly what we observe in figure 6, where tip-splitting is maximal in the flat case ($\beta = 1$), and vanishes as β tends to zero. In addition, it is worth noting that the cylindrical cell case discussed in [20] can be readily obtained from the conical cell situation by taking the limit $\beta \to 0$, and $R \to \infty$, such that $\beta R \equiv a$, $Q/(2\pi a) \equiv v_\infty$ and $n/a \equiv k$ remain constant, where a is the radius of the cylindrical cell, v_∞ is the flow velocity at infinity and k denotes the wave number of the disturbance. By inspecting figure 6 we note that tip-splitting does not occur in such a cylindrical cell limit. This fact is consistent with the findings of [20], where finger tip-splitting has not been detected in cylindrical Hele–Shaw cells. Finally, note that figure 6 interpolates both zero curvature limits: on the far left we have the cylindrical cell limit, with no tip-splitting, and on the far right, the flat cell limit with maximum tip-splitting. In conical geometry the parameter β, which describes the cone apex curvature, also regulates 'the availability of space' for the interface to grow. In contrast, under similar dynamical circumstances, in spherical and cylindrical geometries, due to their natural space restrictions, splitting of the fingers would be inhibited.

Now we turn our attention to the analysis of how changes in β influence finger competition. We consider the influence of a fundamental mode n, assuming n is even, on the growth of its sub-harmonic mode $n/2$. Following steps similar to those performed in the previous tip-splitting discussion, we obtain the following equations of motion for the sub-harmonic

$$\dot{a}_{n/2} = \left\{\lambda(n/2) + \tfrac{1}{2}C(n/2)a_n\right\} a_{n/2} \tag{21}$$

$$\dot{b}_{n/2} = \left\{\lambda(n/2) - \tfrac{1}{2}C(n/2)a_n\right\} b_{n/2} \tag{22}$$

where the finger competition function is defined as

$$C(n/2) = \left[F\left(-\frac{n}{2}, \frac{n}{2}\right) + \lambda(n/2)G\left(\frac{n}{2}, -\frac{n}{2}\right)\right]. \tag{23}$$

The function $C(n/2)$ dictates finger competition behaviour. Observing equations (21) and (22) we verify that $C(n/2) > 0$ increases the growth rate of the cosine sub-harmonic $a_{n/2}$, while inhibiting growth of its sine sub-harmonic $b_{n/2}$. In this case, there exists an increased variability among the lengths of fingers of the less viscous fluid 1 penetrating into the more viscous fluid 2. This effect, which is more intense for larger values of

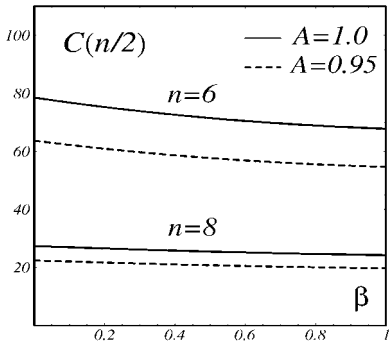

Figure 7. Variation of $C(n/2)$ as a function of β, for Fourier modes $n = 6, 8$. The solid (dashed) curves describe evolution for $A = 1$ ($A = 0.95$).

$C(n/2)$, breaks the n-fold rotational symmetry of the fundamental, and therefore describes finger competition.

To illustrate how finger competition varies with the cell opening angle, in figure 7 we plot $C(n/2)$ as a function of β. In this case, we consider a particular v and L combination at the onset of growth of mode n (using the condition $\lambda(n) = 0$) in the flat cell limit, where it is known that $C(n/2) > 0$ [18]. We see from figure 7 that, for a specific n, finger competition increases for smaller values of β. This indicates that, if fingers grow in a conical cell of small opening angle, they will compete more strongly. In contrast, if the cell is wide enough, the fingers will have ample space to grow with a significant smaller competition. In addition, we observe that the larger the number of fingers, the weaker the competition. The sensitivity of $C(n/2)$ with respect to changes in A is more evident for smaller values of β and n.

We conclude this section by briefly discussing the case $\beta > 1$. In this case, instead of removing a wedge of an initially smooth, flat background to get an ordinary cone, one would insert a wedge into it. We consider that β is just slightly greater than 1, resulting in a gently rippled, cone-like surface presenting small bumps, due to the 'excess angle' induced by the insertion of a wedge. Such a surface is still perfectly described by metric (1). Interestingly, if $\beta > 1$ the Gaussian curvature concentrated at the vertex of the cone-like surface becomes *negative*. Since flow in porous media and in Hele–Shaw cells seems to be linked to flow in negatively curved surfaces [19], it is instructive to investigate what are the effects of $\beta > 1$ on tip-splitting and finger competition. In [19] it has been shown that $K < 0$ enhances tip-splitting. In order to investigate these issues more quantitatively we performed Taylor expansions of both $T(2n, n)$ and $C(n/2)$, considering values of $\beta = 1 + \epsilon$, where $\epsilon \ll 1$. Our results show that $\beta > 1$ enhances tip-splitting and diminishes finger competition in comparison to the case $0 < \beta \leqslant 1$. The present study for $\beta > 1$ is complementary to previous analysis of flow on *uniformly* curved surfaces with $K < 0$ [19], in the sense that we predict how both finger tip-splitting and competition behave on *locally flat* surfaces presenting a conical singularity with a $K < 0$ signature.

4. Conclusions

Motivated by the success of the geometric theory of defects developed by Katanaev and Volovich [1] in dealing with problems in gravitation and condensed matter, we apply a similar geometric approach to fluid mechanics. We have studied viscous flow and pattern formation in a conical Hele–Shaw cell. Such a conical background space has the unique feature of being

locally flat, but not globally equivalent to standard planar Hele–Shaw cells. We have explored the effects of the cell's peculiar geometrical and topological features on the dynamic evolution of the emerging interfacial patterns. Our analytical approach connects the nontrivial structure of the conical cell to a single topological parameter, amenable to laboratory experimentation: the cell's opening angle.

We used a perturbative mode-coupling analysis and derived a nonlinear differential equation which describes the time evolution of the interface perturbation amplitudes up to second-order accuracy. For fixed cell angles, we found that nonlinear effects lead to patterns presenting evident finger tip-splitting and finger competition. Variation of the cell opening angle leads to remarkable changes in the interface behaviour: increasingly larger angles lead to enhanced tip-splitting and diminution of finger competition. In conclusion, we have shown that the geometry and topology of the conical cell couples to the flow dynamics causing significant modifications in the interface shape. The cell opening angle regulates interfacial morphology and can be used as a parameter to control both tip-splitting and competition of the viscous fingers.

Acknowledgments

We thank CNPq (through its PRONEX Program) and CAPES (PROCAD) for financial support. We acknowledge useful discussions with Fernando Parisio and Claudio Furtado.

References

[1] Katanaev M O and Volovich I V 1992 *Ann. Phys., NY* **216** 1
[2] Kleinert H 1989 *Gauge Fields in Condensed Matter* (Singapore: World Scientific)
[3] Heeger A J 1981 *Commun. Solid State Phys.* **10** 53
[4] Kleman M 1983 *Points, Lines and Walls* (New York: Wiley)
[5] Moraes F 2000 *Braz. J. Phys.* **30** 304
[6] Poénaru V 1981 *Commun. Math. Phys.* **80** 127
[7] Furtado C and Moraes F 1997 *Class. Quantum Grav.* **14** 3425
[8] Bausch R, Schmitz R and Turski L A 1998 *Phys. Rev. Lett.* **80** 2257
[9] de Pádua A, Parisio-Filho F and Moraes F 1998 *Phys. Lett.* A **238** 153
[10] Azevedo S, Furtado C and Moraes F 1998 *Phys. Status Solidi* b **207** 387
[11] Katanaev M O and Volovich I V 1999 *Ann. Phys., NY* **271** 203
[12] Ribeiro C A D, Furtado C, Bezerra V B and Moraes F 2001 *J. Phys. A: Math. Gen.* **34** 6119
[13] Lazar M 2002 *J. Phys. A: Math. Gen.* **35** 1983
[14] Saffman P G and Taylor G I 1958 *Proc. R. Soc.* A **245** 312
[15] Bensimon D, Kadanoff L P, Liang S, Shraiman B I and Tang C 1986 *Rev. Mod. Phys.* **58** 977
McCloud K V and Maher J V 1995 *Phys. Rep.* **260** 139
[16] Paterson L 1981 *J. Fluid Mech.* **113** 513
[17] Miranda J A and Widom M 1998 *Int. J. Mod. Phys.* B **12** 931
[18] Miranda J A and Widom M 1998 *Physica* D **120** 315
[19] Parisio F, Moraes F, Miranda J A and Widom M 2001 *Phys. Rev.* E **63** 036307
[20] Miranda J A 2002 *Phys. Rev.* E **65** 026303
[21] do Carmo M P 1977 *Differential Geometry of Curves and Surfaces* (New York: Prentice-Hall)
[22] Dubrovin B A, Fomenko A T and Novikov S P 1984 *Modern Geometry—Methods and Applications, Parts 1 and 2* (New York: Springer)
[23] Sokolov D D and Starobinskii A A 1977 *Sov. Phys. Dokl.* **22** 312
[24] Tavares D M and Romero C 1998 *Mod. Phys. Lett.* A **13** 2077
[25] Landau L D and Lifshitz E M 1987 *Fluid Mechanics* (New York: Pergamon)